Dynamics of a thin twisted flux tube

D. W. Longcope
Department of Physics, Montana State University, Bozeman, MT 59717

I. Klapper
Department of Mathematical Sciences, Montana State University, Bozeman, MT 59717

ABSTRACT

A set of dynamical equations are derived for a slender tube of isolated magnetic flux generalizing a model due to Spruit. The tube is assumed to consist of field lines which twist about the tube's axis at some rate q. The equations describe the evolution of the axis and the evolution of the twist. They include the interaction between twist and motions of the axis described as writhing. Through this interaction the motion of the axis can introduce twist into a previously untwisted tube. The twist so introduced will have a sign opposite to the local handedness of the axial curve. This may be important for the generation of current in emerging active regions. Tubes with sufficiently large twist are subject to an instability which distorts the axis into a helix of pitch similar to the tubes field lines. Such an instability might be responsible for observed morphology in δ-spots on the Sun.

1. Introduction

At the photosphere the solar magnetic field is concentrated into isolated elements, which are in turn grouped into active regions. The prevailing understanding of this morphology holds that the magnetic field rises through the Sun's convective zone (CZ) in the form of thin isolated strands known as *flux tubes* (see e.g. Parker 1979). The nonlinear dynamics of a thin magnetic flux tube was modeled by Spruit (1981) in a form which has been used subsequently by many investigators (Moreno-Insertis 1986, Choudhuri and Gilman 1987, Chou and Fisher 1989, D'Silva and Choudhuri 1993, Fan et al. 1993). Numerical simulations of Spruit's equations suggest that a flux tube rises from the base of the CZ in about two to three months. There are many aspects of these simulations which agree with observation including the asymmetric proper motions (Caligari et al. 1995) and field strengths (Fan et al. 1993) of emerging bipoles. The tilt angles of simulated bipoles also agree with observations in their latitude dependence (D'Silva and Choudhuri 1993), flux dependence (Fan et al. 1994, Fisher et al. 1995), and statistical scatter (Longcope and Fisher 1996).

Spruit's model follows from applying equations of ideal MHD to a slender tube of flux. The tube is assumed slender (thin) in the sense that its cross sectional radius a is negligible in relation to both the atmospheric scale height, and any scales of variation along the tube. The dynamical equations are the lowest order in an expansion of MHD in powers of a/L, where L is any of the global length scales.

In derivations of the model equations it is customary to assume that the tube consists of *untwisted* flux, meaning that every magnetic field line is roughly parallel to the axis of the tube. Assuming instead that the field lines twist about the axis, winding once over an axial length L_w, contributes additional terms to the axis dynamics which scale as a^2/L_w^2 (Feriz-Mas and Shussler 1990). If L_w is comparable to global length scales, such as the atmospheric scale height, then this contribution is neglected in the course of passing to the thin limit; we refer to this as the *weakly twisted* regime (Linton et al. 1996). Thus Spruit's model, while appearing to apply only to untwisted flux tubes, actually applies to weakly twisted flux tubes as well.

It has been noted that the presence of some twist is essential in formulating a self-consistent picture of a flux tube. Without twist a real flux tube would lack integrity and would not behave as a single object for very long (Parker 1979). Linear analysis (Tsinganos 1980) and numerical simulations (Schussler 1979, Longcope et al. 1996) confirm that a truly untwisted magnetic flux tube is quickly fragmented by hydrodynamic forces. By twisting about the axis, field lines provide a tension which may be adequate to prevent this fragmentation (Moreno-Insertis and Emonet 1996).

There is mounting observational evidence that emerging flux tubes are indeed twisted. Vector magnetograms have provided ample evidence that the coronal magnetic field carries current. Recently Leka et al. (1996) showed that this current increases in rough proportion to the flux during the period of emergence. This was interpreted as an indication that the flux tube was carrying current (i.e. had twisted field lines) prior to emergence. The inherent twist in emerging field may prove to be one of the fundamental features of the solar dynamo. Pevtsov et al. (1995) found, in a sample of 69 active regions, that those in the northern (southern) hemisphere showed a strong tendency to have a left-handed (right-handed) sense of twist. This intrinsic twist should be distinguished from the handedness induced by the Coriolis force (Joy's law) which has a sign opposite to that found by Pevtsov et al.

To interpret such observations it would help to develop a flux tube model which explicitly includes twist. We derive such a model in this paper. It consists of an equation for the dynamical evolution of the tube's axis (akin to Spruit's) as well as equations for the time evolution of the twist. The derivation employs the thin tube assumption $a/L \ll 1$ but is not restricted to weak twisting. To retain the contributions from even weak twist self-consistently it will be necessary to retain terms of the next-highest order in a/L. In the weakly twisted regime, however, the nighest order terms in the axis dynamics corresponds to Spruits model as discussed

above. Even in this case the twist dynamics depend on the evolution of the axis; we call this a case of passive twist.

In a tube with strong twist ($a \sim L_w$) the dynamics of the axis can be affected, or even driven by the twist. One example is offered by the helical kink mode which has been extensively studied in tubes with initially straight axes (see e.g. Linton et al. 1996). The instability causes the axis of the tube to distort into a helix whose pitch is similar to that of the individual field lines. If such an instability were to occur in a rising flux tube it would lead to behavior that cannot be described by Spruit's equations. Observations of sun-spots emerging in the *island-δ* configuration have been interpreted as flux tubes whose axes formed loops (Tanaka 1991). It has been suggested that the island-δ configuration results from the nonlinear evolution of a helical kink mode (Linton et al. 1996).

Attempts to generalize Spruit's derivation directly by formal expansions of the velocity and magnetic fields as a series in radius from the axis ϖ have not lead to usable nonlinear equations (Ferriz-Mas and Schussler 1990, Lau 1995). By contrast, dynamical equations have recently been derived for thin, twisted elastic rods (Klapper 1996, Dichmann and Maddocks 1996) which bear a formal similarity to flux tubes. In particular elastic rods are susceptible to a dynamical instability, the *writhing instability*, which resembles the helical kink mode. Rather than an expansion of fields these equations are derived using integrated force and moment balances. In this paper we will apply similar techniques to equations of ideal MHD to derive equations for a thin, twisted flux tube.

In Section 2 we define twist and derive a kinematic equation for its evolution on a moving flux tube. This equation is a very general one containing the effects of topological constraints and applies to other systems such as ribbons or rods. In Section 3 we use the equations of MHD to find forces and torques on a flux tube. This results in dynamical equations for the tube's axis and for the self-consistent evolution of twist. The latter consists of two equations which describe the propagation of torsional Alfvén waves. Finally, in Section 4 we apply the dynamical equations to the example of a uniformly twisted tube with a helical axis. The interaction of the twist and helical pitch lead to nontrivial behavior including a helical kink mode which has saturated nonlinearly. In addition we show that a helical distortion of the tubes axis introduces twist of opposing sign. Applying this to a conceptual picture of an emerging flux tubes predicts measurements with the same sign, but smaller by a factor of three, than those made by Pevtsov et al. (1995).

2. Kinematics of twisted tubes

2.1. Evolution of twist

This section concerns the kinematics of a tube whose cross-section is a circle of radius $a(\ell)$ centered on a curve $\mathbf{x}(\ell)$, called its axis, where ℓ is arclength. The tube is made up of magnetic field lines and it is assumed that there is no magnetic field outside the tube. The vector $\hat{\mathbf{l}} = d\mathbf{x}/d\ell$ is the unit tangent vector to $\mathbf{x}$ and we define $\mathbf{k} = d\hat{\mathbf{l}}/d\ell$ to be the curvature vector of $\mathbf{x}$. The quantity $\kappa = |\mathbf{k}|$ is the curvature of $\mathbf{x}$ (κ is the reciprocal of the local radius of curvature) and $\hat{\mathbf{n}} = \kappa^{-1}\mathbf{k}$ is the Frenet normal vector to $\mathbf{x}$. At points where $\kappa \neq 0$ we can define the binormal vector $\hat{\mathbf{b}} = \hat{\mathbf{l}} \times \hat{\mathbf{n}}$ (fig. 1).

In addition to the axis our model will describe the other field lines in the tube. Any such field line will trace out a curve $\mathbf{x}(\ell) + r\boldsymbol{\xi}(\ell)$ where $r \leq a$ and $\boldsymbol{\xi}$ is a unit vector perpendicular to $\hat{\mathbf{l}}$. Figure 2 shows a field line on the outside of the flux tube, $\mathbf{x}(\ell) + a\boldsymbol{\xi}(\ell)$.This field line is said to *twist* about the axis with a pitch q if $\partial\boldsymbol{\xi}/\partial\ell = q\hat{\mathbf{l}} \times \boldsymbol{\xi}$, at least for a straight axis. In general, each field line in a tube can twist about the axis with a different pitch, however, we are going to restrict our consideration to tubes in which every field line has the same pitch $q(\ell)$ at a given axial position ℓ. We discuss the consistency of such a restriction below, but for now we are concerned only with kinematics.

The unit vector $\boldsymbol{\xi}$ simultaneously twists about $\hat{\mathbf{l}}$ and remains normal to it. To do this it must satisfy the equation

$$\frac{d\boldsymbol{\xi}}{d\ell} = \boldsymbol{\Lambda} \times \boldsymbol{\xi} = \left[q\hat{\mathbf{l}} + \hat{\mathbf{l}} \times \frac{\partial \hat{\mathbf{l}}}{\partial \ell}\right] \times \boldsymbol{\xi} \quad . \tag{1}$$

The tangential component of $\boldsymbol{\Lambda}$ is the definiton of twist q, the nontangential component enforces $\boldsymbol{\xi} \cdot \hat{\mathbf{l}} = 0$. The field line traced by $\boldsymbol{\xi}$ will move as the flux tube evolves so $\boldsymbol{\xi}$ must evolve in time. By analogy to eq. (1) this time evolution is governed by

$$\frac{d\boldsymbol{\xi}}{dt} = \boldsymbol{\Omega} \times \boldsymbol{\xi} = \left[\omega\hat{\mathbf{l}} + \hat{\mathbf{l}} \times \frac{d\hat{\mathbf{l}}}{dt}\right] \times \boldsymbol{\xi} \tag{2}$$

where the *spin* $\omega(\ell)$ is the local rotation rate of the flux tube about its axis.

Our aim in this section is to derive an evolution equation for $q(\ell)$ given prescribed functions $\omega(\ell, t)$ and $\mathbf{x}(\ell, t)$. To do this we follow the derivation in Klapper and Tabor (1994). Consider a short length $d\ell$ of flux tube from $\mathbf{x}(\ell)$ to $\mathbf{x}(\ell + d\ell)$. Over that length the vector $\boldsymbol{\xi}$ rotates through an angle $d\theta = qd\ell$. We divide the tube motion into two pieces and treat the effect on q of each separately. First if the curve $\mathbf{x}$ remains fixed and $\boldsymbol{\xi}$ rotates around $\hat{\mathbf{l}}$, i.e., $d\hat{\mathbf{l}}/dt = d(d\ell)/dt = 0$

and $\boldsymbol{\Omega} = \omega\hat{\mathbf{l}}$, then

$$\begin{aligned}\frac{d}{dt}(q\ d\ell) &= \frac{d}{dt}(d\theta) = [\boldsymbol{\Omega}(\ell + d\ell) - \boldsymbol{\Omega}(\ell)] \cdot \hat{\mathbf{l}}(\ell) \\ &= \omega(\ell + d\ell) - \omega(\ell) + O(d\ell^2) \end{aligned} \tag{3}$$

so in this case

$$\frac{dq}{dt} = \frac{\partial \omega}{\partial \ell} \quad . \tag{4}$$

Secondly, if we consider the remaining non-spinning component of flux tube motion, i.e., $\omega = 0$, then

$$\begin{aligned}\frac{d}{dt}(qd\ell) &= \frac{d}{dt}(d\theta) = [\boldsymbol{\Omega}(\ell + d\ell) - \boldsymbol{\Omega}(\ell)] \cdot \hat{\mathbf{l}}(\ell) \\ &= \boldsymbol{\Omega}(\ell + d\ell) \cdot \hat{\mathbf{l}}(\ell) = \left(\hat{\mathbf{l}}(\ell + d\ell) \times \frac{d\hat{\mathbf{l}}}{dt}(\ell + d\ell)\right) \cdot \hat{\mathbf{l}}(\ell) \\ &= \left(\frac{\partial \hat{\mathbf{l}}}{\partial \ell} \times \frac{d\hat{\mathbf{l}}}{dt}\right) \cdot \hat{\mathbf{l}}(\ell)\ d\ell + O(d\ell^2) \quad . \end{aligned} \tag{5}$$

Thus the non-spinning component of motion results in a change in twist q according to

$$\frac{dq}{dt} = -\zeta q + \left(\frac{\partial \hat{\mathbf{l}}}{\partial \ell} \times \frac{d\hat{\mathbf{l}}}{dt}\right) \cdot \hat{\mathbf{l}}(\ell) \tag{6}$$

where $\zeta = (d/dt)\ln(d\ell)$ is the local logarithmic rate of change of arclength (note that stretching the axis $\mathbf{x}$ reduces twist). Defining the velocity of the axis as a Lagrangian derivative $\mathbf{v} = d\mathbf{x}/dt$ allows ζ to be expressed

$$\zeta \ = \ \frac{d\ln(dl/d\mu)}{dt} \ = \hat{\mathbf{l}} \cdot \frac{\partial \mathbf{v}}{\partial \ell} \quad , \tag{7}$$

where μ is a Lagrangian coordinate. Combining equations (4) and (6) we observe that a general proscribed motion consisting of both velocity $\dot{\mathbf{x}}$ and spin ω induces

$$\frac{dq}{dt} = -\zeta q + \frac{\partial \omega}{\partial \ell} + \left(\frac{\partial \hat{\mathbf{l}}}{\partial \ell} \times \frac{d\hat{\mathbf{l}}}{dt}\right) \cdot \hat{\mathbf{l}} \quad . \tag{8}$$

This coupling equation between twist, spin, and curve motion is the main result of this section. The last term on the right-hand side (rhs),

$$\left(\frac{\partial \hat{\mathbf{l}}}{\partial \ell} \times \frac{d\hat{\mathbf{l}}}{dt}\right) \cdot \hat{\mathbf{l}} = \kappa\hat{\mathbf{b}} \cdot \frac{d\hat{\mathbf{l}}}{dt} \quad ,$$

couples the "writhing" motion of $\mathbf{x}$ to change in the flux tube twist q. Note that $\kappa\hat{\mathbf{b}} \cdot (d\hat{\mathbf{l}}/dt)$ = (curvature)×(rotation of $\mathbf{x}$ into the binormal direction), the local change in "helical-ness" of $\mathbf{x}$ (Klapper and Tabor 1994).

2.2. Helicity of a thin twisted flux tube

We consider a thin tube $\mathcal{B}$ of magnetic field lines with the simple structure described in the previous section. In the absence of magnetic diffusivity, the helicity $H = \int_{\mathcal{B}} \mathbf{A} \cdot \mathbf{B}\, dx^3$ of this tube is conserved. For the helicity to be well defined the flux tube $\mathcal{B}$ should be closed (Moffatt 1978). It has been observed (Berger and Field 1984, Moffatt and Ricca 1992) that for this simple geometry H can be divided into two pieces called the *writhe helicity* Wr and the *twist helicity* Tw. (H can be interpreted as, roughly, the average linkage Lk of pairs of magnetic field lines, a conserved quantity, and the relation $H = Tw + Wr$ is analogous to the relation $Lk = Tw + Wr$ known to hold for the edges of a ribbon [Calugareanu 1961, Pohl 1968, White 1969].) Tw is defined by the integral

$$Tw(q) = \frac{\Phi^2}{2\pi} \oint q d\ell \tag{9}$$

where Φ is the magnetic flux through a tube cross-section. The writhe helicity Wr, a measure of "helical-ness" of the curve $\mathbf{x}$, is defined by the integral

$$Wr(\mathbf{x}) = \frac{\Phi^2}{4\pi} \oint \oint \frac{\hat{\mathbf{l}}(\ell_1) \times \hat{\mathbf{l}}(\ell_2)}{|\mathbf{x}(\ell_1) - \mathbf{x}(\ell_2)|^2} \cdot \frac{\mathbf{x}(\ell_1) - \mathbf{x}(\ell_2)}{|\mathbf{x}(\ell_1) - \mathbf{x}(\ell_2)|} d\ell_1 d\ell_2. \tag{10}$$

Note that Tw is defined by a single integral and thus has a local density, namely $q\, d\ell$, while Wr is defined by a double integral and hence has no local density. That is, Wr depends on the global geometry of $\mathbf{x}$ and cannot in general be calculated by independently adding contributions from individual short sections of $\mathbf{x}$.

As will be seen in Section 4, the twist q is related to the magnetic energy of the flux tube and a reduction in the magnitude of q might result in a reduction in energy. Due to the conservation of helicity and the relation $H = Tw + Wr$, in general a reduction in twist will result in an increase in Wr. Thus the change in writhe will have the opposite sign as the change in Tw. This opportunity to change twist into writhe and decrease the energy may result in *writhing instabilities* where the axis forms helical structures.

At first glance its nonlocal nature makes Wr an inconvenient diagnostic since its determination requires a knowledge of the entire geometry of $\mathbf{x}$. The important quantity for studying stability, however, is the change of writhe ΔWr, and this quantity does have a local density. That is, ΔWr can be calculated by adding contributions from short lengths of $\mathbf{x}$ independent of the rest of the curve $\mathbf{x}$. To see this, note that $\dot{H} = 0$ so that $\dot{Wr} = -\dot{Tw}$. Time differentiating eq. (8) and using expressions (3) and (5)

$$\frac{d}{dt} Tw = \frac{\Phi^2}{2\pi} \oint \frac{d}{dt}(q d\ell) = \frac{\Phi^2}{2\pi} \oint \left[\frac{\partial \omega}{\partial \ell} + \left(\frac{\partial \hat{\mathbf{l}}}{\partial \ell} \times \frac{d\hat{\mathbf{l}}}{dt} \right) \cdot \hat{\mathbf{l}} \right] d\ell$$

$$= \frac{\Phi^2}{2\pi}\oint\left(\frac{\partial\hat{\mathbf{l}}}{\partial\ell}\times\frac{d\hat{\mathbf{l}}}{dt}\right)\cdot\hat{\mathbf{l}}\,d\ell \quad ,$$

so that

$$\frac{d}{dt}Wr = -\frac{\Phi^2}{2\pi}\oint\left(\frac{\partial\hat{\mathbf{l}}}{\partial\ell}\times\frac{d\hat{\mathbf{l}}}{dt}\right)\cdot\hat{\mathbf{l}}\,d\ell \quad . \tag{11}$$

Note that this expression is a single integral, even though the definition of Wr involved a double integral. Thus $\dot{Wr}$ has a local density and if only a portion of the flux tube evolves then only that portion will contribute to $\dot{Wr}$. For that matter, it is not necessary for the flux tube to truly be closed for $\dot{Wr}$ to be well defined according to eq. (11). This final observation is related to the notion of relative helicity (Berger and Field 1984) and it implies that it is sensible to discuss a writhing instability for portions of an entire flux tube.

3. Dynamics of twisted tube

3.1. Forces on the tube

To introduce the dynamics of a tube's axis we will consider the forces and torques acting on a short segment V of the tube shown in fig. 1. The tube segment V encompasses a length $d\ell$ of the axis, and is bounded by cross sections of the tube $\Sigma_- = \Sigma(\ell)$ and $\Sigma_+ = \Sigma(\ell + d\ell)$. We will assume that cross-sections always remain unsheared (i.e., intersect the axis $\mathbf{x}(\ell)$ perpendicularly) and also follow the internal motions (i.e. they are impermeable). We will assume that the radius a of the tube is small compared to the radius of curvature of the axis κ^{-1}, and to the pressure scale height H_p of the atmosphere. Finally, we will assume the parameter $\beta = 8\pi p/b^2 \gg 1$ as it is belived to be in the CZ ($\beta \sim 10^5$ at the base).

The force density acting on the interior of V is that from ideal MHD

$$\mathbf{f} = -\nabla\left(\,p + \frac{B^2}{8\pi}\,\right) \;+\; \frac{1}{4\pi}\,(\mathbf{B}\cdot\nabla)\mathbf{B} \;+\; \rho\mathbf{g} \quad . \tag{12}$$

Following Spruit (1981) we will assume that because $a \ll H_p$ pressure balance is always maintained across the tube's diameter

$$p + \frac{B^2}{8\pi} = p_e(z) \quad , \tag{13}$$

where p_e is the external pressure and z is the vertical coordinate (i.e parallel to gravity). Th The external atmosphere is taken to be in hydrostatic equilibrium, $\nabla p_e = \rho_e\,\mathbf{g}$, so the internal force density reduces to

$$\mathbf{f} = \nabla\cdot\left(\,\frac{1}{4\pi}\,\mathbf{BB}\,\right) \;+\; (\rho - \rho_e)\mathbf{g} \quad . \tag{14}$$

The total force acting on a tube segment V is found by integrating this force density

$$\mathbf{F} \;=\; \int_V \mathbf{f}\, d^3r \;=\; \frac{1}{4\pi}\oint_{\partial V} \mathbf{B}(\mathbf{B}\cdot\hat{\boldsymbol{\sigma}})\, d^2r \;+\; (\bar{\rho}-\rho_e)\mathbf{g}\int_V d^3r \quad , \tag{15}$$

where $\hat{\boldsymbol{\sigma}}$ is the outward normal to V, and $\bar{\rho}$ is the average internal density. The only pieces of ∂V for which $\hat{\boldsymbol{\sigma}}\cdot\mathbf{B}$ does not vanish are the cross sections $\Sigma_\pm$ on which $\hat{\boldsymbol{\sigma}} = \pm\hat{\mathbf{l}}$ respectively. Writing the integrated stress on the cross section $\Sigma(\ell)$ as

$$\mathbf{N}(\ell) \;\equiv\; \frac{1}{4\pi}\int_{\Sigma(\ell)} \mathbf{B}(\mathbf{B}\cdot\hat{\mathbf{l}})\, d^2r \quad , \tag{16}$$

allows the net force to be expressed to lowest order in $d\ell$ as

$$\mathbf{F} = \left\{ \frac{\partial \mathbf{N}}{\partial \ell} \;+\; A(\bar{\rho}-\rho_e)\mathbf{g} \right\} d\ell \quad , \tag{17}$$

where $A(\ell) = \pi a^2(\ell)$ is the area of $\Sigma(\ell)$.

Since the mass $dm = \bar{\rho} A\, d\ell$ of V is constant in time the inertia $\mathbf{F}_{\rm I}$ of the tube segment in V is

$$\mathbf{F}_{\rm I} = \frac{d\bar{\mathbf{v}}}{dt}\,\bar{\rho}\, A\, d\ell \quad , \tag{18}$$

where $\bar{\mathbf{v}}$ is velocity of the center of mass. To lowest order in a the mean velocity $\bar{\mathbf{v}}$ is equal to $\mathbf{v} = \dot{\mathbf{x}}$ the velocity of the axis. There is also be an inertial contribution from the motion of the surrounding medium, the so-called enhanced inertia (Spruit 1981). The correct treatment of this contribution is a source of continuing controversy (Choudhuri 1990; Cheng 1992; Fan et al. 1994), however, it may prove unimportant for realistic situations. To simplify expressions we choose to omit the enhanced inertia entirely. It would be a simple matter to add the appropriate term (whatever it turns out to be) to eq. (18) and repeat the derivation presented below.

As the tube slips through the surrounding medium, assumed at rest, there is an aerodynamic drag acting on the tube's surface (Choudhuri and Gilman 1987). This force involves the interaction of the flux tube and the external medium across a turbulent boundary layer. At very large Reynold's number the drag force takes the form (Batchelor 1967)

$$\mathbf{F}_{\rm D} = -C_{\rm D}\rho_e |\mathbf{v}_\perp| \mathbf{v}_\perp\, a\, dl \quad , \tag{19}$$

where $\mathbf{v}_\perp$ is the perpendicular component of the tube's axis velocity, and $C_{\rm D} \simeq 1$ is the drag coefficient. To simplify expressions we will not include this term in what follows; however, it too could be easily included.

Setting the inertia equal to the force $\mathbf{F}$ gives the equation of motion for the tube's axis

$$\dot{\mathbf{v}} = \frac{1}{A\rho}\partial_\ell \mathbf{N} \;+\; \frac{\rho-\rho_e}{\rho}\,\mathbf{g} \quad , \tag{20}$$

where all quantities are averages over the cross section. We will show below that this expression reduced to Spruit's in the case of an untwisted flux tube.

3.2. Torques on the tube

In order to involve twist in the tube dynamics it is necessary to include the torque acting on V as well as the force. The torque density about the center of mass of V ($\mathbf{r} = 0$) is

$$d\boldsymbol{\tau} \;=\; \mathbf{r} \times \mathbf{f}\, d^3r \quad ,$$

where $\mathbf{f}$ is given in (14). The total torque $\boldsymbol{\tau}$ is found by integrating this expression over V,

$$\boldsymbol{\tau} \;=\; \frac{1}{4\pi} \oint_{\partial V} (\mathbf{r} \times \mathbf{B})(\mathbf{B} \cdot \hat{\boldsymbol{\sigma}})\, d^2r \quad . \tag{21}$$

Once again, the only portions of ∂V for which $\mathbf{B} \cdot \hat{\boldsymbol{\sigma}}$ is non-zero are the cross sections $\Sigma_\pm$. On those surfaces the outward normals are $\hat{\boldsymbol{\sigma}} = \pm\hat{\mathbf{l}}$ and radius vector can be written $\mathbf{r} \;=\; \mathbf{r}_\perp \;\pm\; \frac{1}{2} d\ell\, \hat{\mathbf{l}}$. Thus

$$\begin{aligned} 4\pi\boldsymbol{\tau} \;=\; & \int_{\Sigma_+} (\mathbf{r}_\perp \times \mathbf{B})\, (\mathbf{B} \cdot \hat{\mathbf{l}})\, d^2r_\perp \;+\; \tfrac{1}{2} d\ell \int_{\Sigma_+} (\hat{\mathbf{l}} \times \mathbf{B})\, (\mathbf{B} \cdot \hat{\mathbf{l}})\, d^2r_\perp \\ & - \int_{\Sigma_-} (\mathbf{r}_\perp \times \mathbf{B})\, (\mathbf{B} \cdot \hat{\mathbf{l}})\, d^2r_\perp \;+\; \tfrac{1}{2} d\ell \int_{\Sigma_-} (\hat{\mathbf{l}} \times \mathbf{B})\, (\mathbf{B} \cdot \hat{\mathbf{l}})\, d^2r_\perp \quad . \end{aligned} \tag{22}$$

The integrated cross sectional torque is defined as

$$\mathbf{M}(\ell) \;\equiv\; \frac{1}{4\pi} \int_{\Sigma(\ell)} (\mathbf{r}_\perp \times \mathbf{B})\, (\mathbf{B} \cdot \hat{\mathbf{l}})\, d^2r_\perp \tag{23}$$

where the origin of $\mathbf{r}_\perp$ is the center of $\Sigma(\ell)$ (i.e the tube's axis). With this definition the total torque becomes

$$\boldsymbol{\tau} \;=\; \left(\partial_\ell \mathbf{M} \;+\; \hat{\mathbf{l}} \times \mathbf{N} \right) d\ell \tag{24}$$

to lowest order in $d\ell$.

The angular inertia V segment will be denoted $\dot{\mathbf{L}}\, \bar{\rho}\, A\, d\ell$ where $\mathbf{L}$ is an average angular momentum per unit mass. Setting this equal to the torque yields

$$\dot{\mathbf{L}} \;=\; \frac{1}{\rho A} \left(\partial_\ell \mathbf{M} \;+\; \hat{\mathbf{l}} \times \mathbf{N} \right) \quad . \tag{25}$$

The $\hat{\mathbf{l}}$ component of (25) provides an equation for the evolution of the spin ω (see below). The perpendicular components contain information also contained in eq. (20). This redundancy leads to a kind of constraint relating $\mathbf{M}$ and the perpendicular components of $\mathbf{N}$, namely,

$$\mathbf{N}_\perp = \hat{\mathbf{l}} \times \partial_\ell \mathbf{M} - \rho A\, \hat{\mathbf{l}} \times \dot{\mathbf{L}} \quad , \tag{26}$$

obtained by taking the cross-product of eq. (25) with $\hat{\mathbf{l}}$. We discuss this further below.

3.3. The equations of motion

The conservation of momentum and angular momentum presented above provide the physics necessary to describe the evolution of the flux tube. We intend to describe the *configuration* of the flux tube by its axis $\mathbf{x}(\ell,t)$ and its twist $q(\ell,t)$. Other configurational quantities, e.g. $A(\ell,t)$, $\bar{\rho}(\ell,t)$, can then be recovered using pressure balance (13) and mass conservation exactly as in Spruit's model. The configuration can be advanced using the time derivatives $\mathbf{v}(\ell,t)$ and $\omega(\ell,t)$, which can themselves be advanced using (20) and (25), for a complete solution. To form a closed set of equations, however, we need to express the quantities $\mathbf{L}(\ell,t)$, $\mathbf{M}(\ell,t)$ and $\mathbf{N}(\ell,t)$ in terms of the tube's configuration and time derivatives.

These quantities involve integrals over the tube's cross section of integrands which involve the detailed magnetic field, or mass density profiles. Formulating a closed set of equations therefore involves expressing these profiles purely in terms of the tube's configuration. This is done in the Appendix. The resulting expressions depend on the details of the cross-sectional profile only through two constant parameters γ_0 and γ_2 given in eq. (A5). In the case of a "flat profile", a flux tube whose axial field is constant ($B_\ell = \bar{B}$) when the axis is straight, these parameters are both unity. There is a great deal of freedom selecting these parameters because the magnetic field profile is only weakly constrained by equilibrium constraints in a very high β environment (Linton et al. 1996). By contrast, laboratory plasmas typically have β less than one, and the magnetic profile must satisfy constraints related to force balance. In particular it is difficult, in such circumstances, to arrange for the twist q to be the same on all field lines. This is discussed further in the Appendix.

The required quantities $\mathbf{L}(\ell,t)$, $\mathbf{M}(\ell,t)$ and $\mathbf{N}(\ell,t)$, are found by integration over the cross-section. The axial component of stress is found to be

$$N_\ell \;=\; \frac{A\bar{B}^2}{4\pi}\left[\,\gamma_0 \;+\; \tfrac{1}{2}\kappa^2 a^2 \gamma_2\,\right] \;, \tag{27}$$

where $\bar{B}(\ell) = \Phi/A(\ell)$ is the averaged axial field strength. The cross-sectional torque has one term related to twist and one related to bending; together these yield

$$\mathbf{M} = \frac{\gamma_2 \Phi^2}{8\pi^2}\left[\,q\,\hat{\mathbf{l}} \;+\; \kappa\,\hat{\mathbf{b}}\,\right] \;. \tag{28}$$

The angular momentum per unit mass is

$$\mathbf{L} = \frac{A}{2\pi}\left(\,\omega\hat{\mathbf{l}} \;+\; \tfrac{1}{2}\hat{\mathbf{l}} \times \frac{d\hat{\mathbf{l}}}{dt}\,\right) \;. \tag{29}$$

The final requirement for a closed set of equations is an expression for the perpendicular components of $\mathbf{N}$. In principle, this could be found by integration

over the cross section, as was done for N_ℓ and $\mathbf{M}$. Alternatively we can use (26) which relates $\mathbf{N}_\perp$ to $\mathbf{M}$. This expression also contains a term proportional to $\dot{\mathbf{L}}$ which presents a possible source of inconsistency. So far we have assumed that the field profiles, e.g. $B_\ell(\varpi, \phi)$, depend only on the flux tube's configuration, and *not* on its motion. Since both $\mathbf{N}$ and $\mathbf{M}$ are defined in terms only of the field profiles they will therefore depend on $\mathbf{x}(\ell)$ and not on $\dot{\mathbf{x}}(\ell)$ or on $\ddot{\mathbf{x}}(\ell)$. To be consistent with this assumption we must neglect the final term in eq. (26) to yield

$$\mathbf{N}_\perp = \hat{\mathbf{l}} \times \partial_\ell \mathbf{M} = \frac{\gamma_2 \Phi^2}{8\pi^2} \left[(q - \tau)\kappa \hat{\mathbf{b}} - \partial_\ell \kappa \hat{\mathbf{n}} \right] \quad . \tag{30}$$

Using eq. (29) the neglected inertial term can be estimated to be smaller than this expression by factors of $v^2/\bar{v}_{\rm A}^2$ or $v\omega/\bar{v}_{\rm A}^2\kappa$. For the velocity of a buoyantly rising flux tube $v \sim \bar{v}_{\rm A}\sqrt{a/H_p}$ (Parker1975) and an Alfvén wave of global scale $\omega \sim \bar{v}_{\rm A}/L$ each of these factors is small in the thin flux tube ordering $a \ll H_p, L$. In equation (30) we have introduced the geometrical *torsion* τ (unrelated to the torque $\boldsymbol{\tau}$) defined by $\hat{\mathbf{b}} \cdot (d\hat{\mathbf{n}}/ds) = [\hat{\mathbf{n}} \times (d\hat{\mathbf{n}}/ds)] \cdot \hat{\mathbf{l}}$, i.e., the twist rate of $\hat{\mathbf{n}}$ about $\hat{\mathbf{l}}$. Note that τ is undefined if $\kappa = 0$ but it is easily shown that the quantity $\kappa\tau$ can always be defined if $\mathbf{x}$ is smooth.

Combining the parallel and perpendicular terms of $\mathbf{N}$ results in the expression

$$\mathbf{N} = \frac{\gamma_0 A \bar{B}^2}{4\pi} \hat{\mathbf{l}} \; + \; \frac{\gamma_2 \Phi^2}{8\pi^2} \left[(q - \tau)\kappa \hat{\mathbf{b}} - \partial_\ell \kappa \hat{\mathbf{n}} \; + \; \kappa^2 \hat{\mathbf{l}} \right] \quad , \tag{31}$$

which will be used in everything that follows. The first term, which is purely parallel, is the only one used in traditional untwisted thin flux tube equations. The remaining terms are all contributions arising either from twist ($q \neq 0$) or from departures from thinness formally of the same order as the twist terms.

An equation for the evolution of the spin ω comes from the parallel component of the angular momentum equation. Taking the dot product of eq. (25) with $\hat{\mathbf{l}}$ yields

$$\frac{d}{dt}(\hat{\mathbf{l}} \cdot \mathbf{L}) - \frac{d\hat{\mathbf{l}}}{dt} \cdot \mathbf{L} = \frac{1}{\rho A} \partial_\ell (\mathbf{M} \cdot \hat{\mathbf{l}}) \; - \; \frac{1}{\rho A} \mathbf{M} \cdot \mathbf{k} \quad . \tag{32}$$

According to expressions (28) and (29) the second terms on both the rhs and lhs vanish (recall that $\mathbf{k} = \partial_\ell \hat{\mathbf{l}} = \kappa \hat{\mathbf{n}}$). The remaining terms take the form

$$\dot{\omega} + A^{-1}\dot{A}\,\omega \;\; = \;\; \gamma_2 \bar{v}_{\rm A}^2 \, \partial_\ell q \quad . \tag{33}$$

The term $A^{-1}\dot{A}\,\omega$ results from spin-down of a laterally expanding tube. Combining this with the kinematic relation eq. (8),

$$\frac{dq}{dt} = -\zeta q + \frac{\partial \omega}{\partial \ell} + \left(\frac{\partial \hat{\mathbf{l}}}{\partial \ell} \times \frac{d\hat{\mathbf{l}}}{dt} \right) \cdot \hat{\mathbf{l}}, \tag{34}$$

results in a wave equation for q or ω. This describes the propagation of torsional Alfvén waves (see e.g. Priest 1982, §4.3.1) at a phase speed $\gamma_2^{1/2}\bar{v}_{\rm A}$. The factor of $\gamma_2^{1/2}$ averages the different phase-speeds in a tube whose axial field profile is not flat (i.e. $B_\ell(\varpi) \neq \bar{B}$). These equations are linear in q and ω with source terms including the "writhing contribution" to eq. (8).

Substituting the expression for the cross sectional stress into the momentum equation (20) leads to the formidable equation

$$\begin{aligned}\dot{\mathbf{v}} \;=\; & \bar{v}_{\rm A}^2[\,\gamma_0 + \tfrac{1}{2}\gamma_2 a^2(\kappa^2+\tau^2-q\tau)\,]\mathbf{k} \;+\; \gamma_0\bar{v}_{\rm A}^2\,\hat{\mathbf{l}}\,A\,\partial_\ell A^{-1} \;+\; \frac{\rho-\rho_e}{\rho}\,\mathbf{g} \\ & +\; \tfrac{1}{2}\gamma_2\bar{v}_{\rm A}^2 a^2\{\,[\partial_\ell[(q-\tau)\kappa] - \tau\partial_\ell\kappa\,]\,\hat{\mathbf{b}} \;+\; \tfrac{3}{2}\gamma_2\bar{v}_{\rm A}^2 a^2\kappa\partial_\ell\kappa\,\hat{\mathbf{l}} \quad . \end{aligned} \tag{35}$$

This is the generalization of Spruit's original equation for an untwisted, thin flux tube. In the weakly twisted ($qa \ll 1$) and thin limit ($\kappa a \ll 1$, $a\partial_\ell \ll 1$, etc.) this reduces to

$$\dot{\mathbf{v}} = \bar{v}_{\rm A}^2\mathbf{k} \;+\; \bar{v}_{\rm A}^2\,\hat{\mathbf{l}}\,A\,\partial_\ell A^{-1} \;+\; \frac{\rho-\rho_e}{\rho}\mathbf{g} \quad , \tag{36}$$

where we have taken the field profile to be flat ($\gamma_0 = 1$). Using the pressure balance equation in the form

$$\bar{v}_{\rm A}^2\,A\,\partial_\ell A^{-1} \;=\; \rho^{-1}\partial_\ell(p_e - p) \quad ,$$

returns the traditional Spruit equation except for contributions from enhanced inertia

$$\dot{\mathbf{v}} = -\hat{\mathbf{l}}\rho^{-1}\partial_\ell p \;+\; \bar{v}_{\rm A}^2\mathbf{k} + \hat{\mathbf{l}}(\hat{\mathbf{l}}\cdot\mathbf{g}) + \frac{\rho-\rho_e}{\rho}(\hat{\mathbf{l}}\times\mathbf{g})\times\hat{\mathbf{l}} \quad . \tag{37}$$

Thus, we expect that until the tube is strongly twisted ($qa \sim 1$), or sharply bent ($\kappa a \sim 1$), the evolution of the axis will be only slightly different from an untwisted tube.

4. A helical flux tube

In this section we consider the special case of a flux tube with a helical axis. For a straight flux tube any small perturbation can be decomposed into helical components, which are actually its eigenmodes (Linton et al. 1996). We will show that restricting the nonlinear equations to a single helical pitch results in a self-consistent system. In this treatment the role of gravity will be ignored, and $\hat{\mathbf{z}}$ will be taken to be the direction of the helical axis, not necessarily upwards.

4.1. The geometry

The flux tube's axis has a helical pitch p in the $\hat{\mathbf{z}}$ direction, in addition to its twist q, which is taken to be constant. For a right-handed helix $p > 0$. In cartesian

coordinates the axis is

$$\mathbf{x}(\ell) \;=\; u\ell\hat{\mathbf{z}} \;+\; R\left[\cos(pu\ell)\,\hat{\mathbf{x}} \;+\; \sin(pu\ell)\,\hat{\mathbf{y}}\right] \quad , \tag{38}$$

where R is the amplitude of the helix. Since $|\partial\mathbf{x}/\partial\ell| = 1$ by definition we must have

$$u \;=\; \frac{1}{\sqrt{1+p^2R^2}} \quad . \tag{39}$$

For notational convenience we introduce the unit vectors

$$\hat{\mathbf{r}}(\ell) \;=\; \cos(pu\ell)\,\hat{\mathbf{x}} \;+\; \sin(pu\ell)\,\hat{\mathbf{y}} \tag{40}$$

$$\hat{\boldsymbol{\theta}}(\ell) \;=\; -\sin(pu\ell)\,\hat{\mathbf{x}} \;+\; \cos(pu\ell)\,\hat{\mathbf{y}} \quad , \tag{41}$$

which should not be confused with coordinate directions. In terms of these the Frenet unit vectors are

$$\hat{\mathbf{l}} \;=\; u\hat{\mathbf{z}} \;+\; Rpu\,\hat{\boldsymbol{\theta}}(\ell) \tag{42}$$

$$\hat{\mathbf{n}} \;=\; -\hat{\mathbf{r}}(\ell) \tag{43}$$

$$\hat{\mathbf{b}} \;=\; -Rpu\,\hat{\mathbf{z}} \;+\; u\,\hat{\boldsymbol{\theta}}(\ell) \quad . \tag{44}$$

It is a special property of a helix that its curvature κ and torsion τ are constant

$$\kappa \;=\; p^2u^2R = \frac{p^2R}{1+p^2R^2} \tag{45}$$

$$\tau \;=\; pu^2 = \frac{p}{1+p^2R^2} \quad . \tag{46}$$

In addition we will take $A(\ell)$ to be constant, so that all properties of the flux tube are independent of ℓ.

The amplitude R of the helix will be allowed to vary; as it does so we will assume that the pitch p remains fixed ($\dot{p} = 0$). Furthermore, we will assume that all motions are perpendicular to $\hat{\mathbf{z}}$ so

$$\frac{dz}{dt} = \frac{d(u\ell)}{dt} = 0 \quad .$$

Time differentiating eq. (38) gives the velocity $\mathbf{v}(\ell) = \dot{R}\,\hat{\mathbf{r}}(\ell)$. Finally we will assume that the volume of a tube segment $(z, z+dz)$ does not change (i.e. $\beta \to \infty$) so that

$$A\frac{\partial\ell}{\partial z} \;=\; \frac{A}{u} \;=\; \text{const.} \;=\; A_0 \quad , \tag{47}$$

where $A_0 = \pi a_0^2$ is the cross-sectional area when the axis is straight ($R = 0$).

4.2. Kinematics

With the definitions above all expressions in the dynamical equations can be written in terms of the amplitude R and its derivatives. In particular, the logarithmic extension rate

$$\zeta = \hat{\mathbf{l}} \cdot \frac{\partial \mathbf{v}}{\partial \ell} = u^2 p^2 R \dot{R} = \frac{d}{dt} \ln \sqrt{1 + p^2 R^2} \quad . \tag{48}$$

Using this in eqs. (8) and (33) yields $\omega = 0$ and

$$q(R) \;=\; q_0 u \;+\; pu(u-1) \tag{49}$$

where q_0 is the value of q when the axis is straight. The first term on the rhs, $q_0(d\ell_0/d\ell)$, reflects changes in q due to extension of the axis. The second term, which has a sign opposite to p, is the contribution from writhing, $-d(Wr)/d\ell$.

Equation (49) has important consequences for a flux tube which develops writhe from the interaction of the Coriolis force on a rising tube. To see this we will model the emerged flux tube as half a turn of a helix, whose orientation ($\hat{\mathbf{z}}$) is the solar toroidal direction (see fig. 3). The bipole makes an angle ψ with the toroidal direction which is taken to be positive for the orientation corresponding to Joy's law in the Northern hemisphere (i.e. a right handed helix with $p > 0$). The separation distance between footpoints is denoted d, which can be related to the helical parameters p and R as

$$p \;=\; \frac{\pi \,\mathrm{sgn}(\psi)}{d \cos\psi} \tag{50}$$

$$R \;=\; \tfrac{1}{2} d \sin\psi \quad . \tag{51}$$

We will assume that flux is *untwisted* at the base of the CZ so $q_0 = 0$. This allows eq. (49) to be written

$$qd \;=\; -\frac{\pi \,\mathrm{sgn}(\psi)}{\cos\psi} \left(1 + \frac{\pi^2}{4} \tan^2\psi \right)^{-1/2} \left[1 \;-\; \left(1 + \frac{\pi^2}{4} \tan^2\psi \right)^{-1/2} \right] \quad . \tag{52}$$

This expression has the sign opposite to ψ so one expects field lines with left handed twist in the Northern hemisphere. Furthermore the term in square brackets contributes a $\sim \psi^2$ dependence for small tilt angles.

Rather than q, observations of magnetic fields tend to be cast in terms of the force-free parameter α

$$\alpha \equiv \frac{J_\ell}{B_\ell} = B_\ell^{-1} \varpi^{-1} \frac{\partial}{\partial \varpi} (q \varpi^2 B_\ell) = 2q \;+\; q \, \frac{d \ln(B_\ell)}{d \ln \varpi} \quad . \tag{53}$$

For a flat profile the second term on the rhs vanishes leaving the simple relation $\alpha = 2q$. Using this in eq. (52) and assuming small tilt angles ψ (which is true of angles given by Joy's law)

$$\alpha d \;\simeq\; -\frac{\pi^3 \mathrm{sgn}(\psi)}{4}\,\psi^2 \quad . \tag{54}$$

This predicts that, for bipoles adhering to Joy's law, the measured current should have $\alpha < 0$ ($\alpha > 0$) in the northern (southern) hemisphere. It also predicts a magnitude of $\alpha \sim 2 \times 10^{-9}\,\mathrm{m}^{-1}$ for the typical case of $\psi = 10°$ and $d = 100$ Mm. Pevtsov et al. (1995) find a decided tendency for the sign of α to depend on hemisphere in this manner, but with a typical magnitude $|\alpha| \sim 7 \times 10^{-9}\,\mathrm{m}^{-1}$. This value is about a factor of three greater than our estimate.

4.3. Dynamics

The time evolution of R is found from eq. (20). All of the terms involving ∂_ℓ of a scalar will vanish due to the invariance of the helix. All remaining terms (excepting buoyancy which is neglected) are proportional to $\hat{\mathbf{r}}$ so the restriction to a single helix is self-consistent. The coefficients of $\hat{\mathbf{r}}$ yield

$$\ddot{R} = -\bar{v}_{\mathrm{A}0}^2 \frac{A_0^2}{A^2}\left[\,\gamma_0 \;+\; \frac{\gamma_2}{2\pi} A\,(\kappa^2 \;+\; \tau^2 \;-\, q\tau)\,\right]\kappa \quad , \tag{55}$$

where $\bar{v}_{\mathrm{A}0} = \Phi/(4\pi A_0^2 \rho)^{1/2}$ is the Alfvén speed in the straight tube. Introducing expressions for κ, τ, $q(R)$ and $A(R)$ the the rhs of eq. (55) can be written as $-dW(R)/dR$ where

$$W(R) \;=\; \gamma_0 \bar{v}_{\mathrm{A}0}^2 \left\{\,\tfrac{1}{2}u^{-2} \;-\; \tfrac{1}{2}Q^2\left[\,\tilde{p}^2 u - \tfrac{1}{2}\tilde{p}(1-\tilde{p})u^2 - \tfrac{1}{3}\tilde{p}^2 u^3\,\right]\right\} \quad , \tag{56}$$

in terms of the dimensionless parameters

$$\tilde{p} = \frac{p}{q_0} \quad , \quad Q = q_0 a_0 \sqrt{\frac{\gamma_2}{\gamma_0}} \quad .$$

For large R the potential becomes $W(R) \sim \frac{1}{2}\gamma_0 \bar{v}_{\mathrm{A}0}^2 p^2 R^2$ which is sufficient to keep $R(t)$ finite for all times.

The form of the potential $W(R)$ depends on the parameters Q and $\tilde{p}$. Expanding eq. (56) about $R = 0$ gives

$$W(R) \;\simeq\; W_0 \;+\; \tfrac{1}{2}\gamma_0 \bar{v}_{\mathrm{A}0}^2\left[\,1 - \tfrac{1}{2}Q^2\tilde{p}(1-\tilde{p})\,\right] p^2 R^2 \;+\; \mathcal{O}(p^4 R^4) \quad . \tag{57}$$

The second derivative $W''(0)$ is positive, and the equilibrium is unstable, if $Q < 2\sqrt{2}$; a condition which can be restated as a critical twist

$$q_0 > q_{\mathrm{cr}} = \frac{2\sqrt{2}}{a_0}\sqrt{\frac{\gamma_0}{\gamma_2}} \qquad \text{for instability} \quad ,$$

where a_0 is the radius of the tube. In this case the second derivative is positive for values of p in the range

$$|p - \tfrac{1}{2}q_0| \;<\; \tfrac{1}{2}q_0\sqrt{1 - 8/Q^2} \;=\; \tfrac{1}{2}\sqrt{q_0^2 - q_{\rm cr}^2} \quad . \tag{58}$$

This range of unstable pitches is centered on $p = \frac{1}{2}q_0$, but the peak growth rate occurs above this at

$$p_{\rm max} \;=\; \tfrac{1}{2}\sqrt{2q_0^2 - q_{\rm cr}^2} \quad .$$

Figure 4 shows potentials $W(R)$ for an unstable case ($Q = 4$) plotted for values of p both inside and outside the range of instability.

The infinite straight twisted tube can be taken to approximate the top portion of a rising Ω-loop of flux (i.e. $\hat{\mathbf{y}}$ is upward, for instance). The tube has some intrinsic twist q_0 which will not change much due to the rise; it is only slightly affected by the lengthening of the tube and by the Coriolis force. As it rises, however, the tube will expand so a_0 will be a slowly increasing function of time. It is therefore possible for the tube to go from being stable ($Q < 2\sqrt{2}$) to unstable (Linton et al. 1996). At some point after this transition a small helical perturbation of some pitch p, say $p = \frac{1}{2}q_0$ will occur and grow exponentially. (Alternatively, from a random assortment of perturbations the one whose pitch is closest to $p_{\rm max}$ would probably dominate.) This growth occurs when R slides off the central peak in fig. 4d and into the potential well. It then oscillates about the minimum $R = R^*$ (shown as a triangle) perhaps being damped by some friction or drag effects (not included in our model). Eventually the helix will come to rest at the energy minimum $R = R^*$. In this final state the linear instability has "saturated" and the tube's new equilibrium is a helix of finite amplitude, comparable to $1/q_0$.

The linear instability above, which we will call a *writhing instability*, is similar in character to the helical kink mode found by Linton et al. (1996). There is a critical twist $q_{\rm cr} \sim 1/a_0$ for onset, and tube's axis develops a helical pitch of the same sign as the field lines (i.e. p and q_0 have the same sign). In both cases a tube is unstable to a range of helical pitches, and the extent of the range scales as $\sqrt{q_0^2 - q_{\rm cr}^2}$. For the helical kink mode this range is centered on $p = q_0$ while for the writhing instability it is centered on $p = \frac{1}{2}q_0$. Here we should note that the instabilities arise from very different treatments of the flux tube physics, and need not agree in any respect at all. For instance, the helical kink mode involves motion primarily inside the flux tube, while our model assumes that the flux tube's cross section behaves rigidly. Nevertheless, both instabilities derive their free energy from excessive twist; this energy is decreased by trading some twist for writhe of the tube's axis. The advantage of the thin flux tube formulation above is that it is a nonlinear model and can be easily applied to situations of interest in the Sun.

In the rise scenario above the q_0 remains fixed, while $q_{\rm cr}$ is decreasing due to the

tube's expansion. Once $q_{\rm cr}$ drops below q_0 the tube is unstable with a growth time

$$t_{\rm lin} \;=\; [-W''(0)]^{-1/2} \;\simeq\; \frac{2}{\sqrt{\gamma_0}\bar{v}_{\rm A0}}\,\frac{q_{\rm cr}}{q_0}\,(\,q_0^2 - q_{\rm cr}^2\,)^{-1/2} \quad , \tag{59}$$

where we have taken $\tilde{p} = \frac{1}{2}$. While this starts out very long when $q_0 \simeq q_{\rm cr}$ it decreases until it is much shorter than the rise time (Linton et al. 1996). At this point we can assume that the instability has saturated, and the tube is a helix of amplitude R^*. The dimensionless quantity $q_0 R^*$ is a function of Q and $\tilde{p}$ only (see fig. 5). For the wavenumber of maximum linear growth rate, $\tilde{p}_{\rm max}$, the value of $q_0 R^*$ remains bounded by 1.0088, as shown by the dark solid line in fig. 5. For the pitch $p = \frac{1}{2}q_0$ the bounding amplitude is $q_0 R^* = 5.088$. Except for vanishing pitches ($p \to 0$) there is an upper bound on the value of $q_0 R^*$. This means that the amplitude of the saturated helix is dictated by $1/q_0 \sim a_0$, so the equilibria arising from the writhing instability will have amplitudes of a few tube radii.

5. Discussion

We have presented a set of equations describing the time evolution of a thin, twisted flux tube generalizing the equations of Spruit by the introduction of a new degree of freedom twist, $q(\ell)$, and its rate of change — spin $\omega(\ell)$. The equations for these new variables are torsional Alfvén wave equations on the tube. In addition the equation for the evolution of the tube's axis contains contributions from twist. These contributions are two orders smaller in thinness than the terms from Spruit's equations and so in many circumstances their dynamical consequences will be small. However in cases of strong twisting, $qa \sim 1$, these effects can become significant and the tube becomes unstable to *writhing*. Also, twist-related forces provide a mechanism for out of the plane motion absent from the Spruit model.

The twisted flux tube equations can be applied to calculations in two different regimes. The first is the weakly twisted regime, $qa \ll 1$, which we will call "passive twist". In this case the axial dynamics are not significantly affected by the twist, so the evolution of $\mathbf{x}(\ell, t)$ can be found using the equations originally proposed by Spruit (or by subsequent authors). A typical situation would begin with a closed flux tube encircling the Sun at the base of the CZ. This is perturbed in some way causing a section of the tube to rise to the surface as an Ω-loop (see e.g. Fan et al. 1994). Afterward $\omega(\ell, t)$ and $q(\ell, t)$ can be found from eqs. (8) and (33) for the known axial evolution $\mathbf{x}(\ell, t)$. These equations are linear and inhomogeneous, thus the complete solution can be found by combining two conceptually distinct parts. The first part is the *particular solution* for trivial initial conditions, $q(\ell, 0) = \omega(\ell, 0) = 0$, driven by the source term

$$\left(\frac{d\hat{\mathbf{l}}}{d\ell} \times \frac{d\hat{\mathbf{l}}}{dt}\right) \cdot \hat{\mathbf{l}}$$

appearing on the rhs of eq. (8). As discussed above, this source term represents the introduction of twist due to writhing of the axis. The trivial initial conditions describe a situation where the flux tube at the base of the CZ is untwisted. We expect the source term to be largest at the top of the Ω-loop, where the Coriolis forces cause the loop to "tilt". We showed in Section 4.2 that this contributes a value of q which is negative (positive) in the Northern (Southern) hemisphere, in accordance with observations (Pevtsov et al. 1995). Our simple example, however, did not account for the time evolution of the twist. In the self-consistent evolution described here twist introduced by the Coriolis force would tend to propagate away from the top as a torsional Alfvén wave. For this reason we expect the value of q in eq. (52) to be an over-estimate. Since the value in eq. (54) is already smaller than observed it may turn out that this homogeneous solution is not the full explanation of twist in emerging flux tubes.

The second part of the passive twist calculation involves solving the homogeneous equations (i.e. omit the source term from eq. [8]), but with non-trivial initial conditions. A logical initial condition would be for the flux tube to be uniformly twisted at the base of the CZ, say $q(\ell, 0) = 1$. This represents a scenario where flux tubes are generated with some intrinsic twist. There has been some speculation that emerging flux tubes must be generated with twist in order to rise at all (Longcope et al. 1996). This solution can be scaled and added to the particular solution to give the full solution for arbitrary initial twist. It is this composite value of q which should be compared to the value of α in emerged bipoles. At present nothing definitive can be said about the value of this initial twist. If it is different for each flux tube, however, it would presumably introduce randomness into any relationship between α and ψ such as (53). Comparing these calculations to observations would provide important insight into the initial twistedness of flux tubes.

The passive calculation described above should then be tested against the condition that the twist is weak $qa \ll 1$. Specifically, one could test the local stability against writhing $qa < 2\sqrt{2}$ to determine the true passivity of twist. If this were to be violated anywhere that would presumably be at the top of the tube. Such a case would need to be treated with the full set of dynamical equations including (20). The results of sec. 4.3 suggest that the linear instability will saturate in a tube whose axis is deformed. In a straight tube the axis deforms into a helix of pitch similar to the initial twist, and amplitude comparable to the tube's radius. Such a configuration is not, strictly speaking, describable as "thin". We similarly expect the top portion of a flux tube which has undergone the writhing instability to be knotted over a radius comparable to the cross-sectional radius. While the dynamical equations are not strictly valid in this regime their solution might indicate how the "thick" flux tube will behave.

To derive a closed set of equations for a non-thin tube it was necessary to

consider a constrained form of flux tube motion. Unshearability is the assumption that the cross sections of the flux tube remain perpendicular to the axis. The restriction eliminates axial shear motions which are actually known to be part of the helical kink mode (Linton et al. 1996), however, these would require at least one more degree of freedom. Further restrictions on the internal dynamics are also necessary in order to truncate the number of degrees of freedom. For this reason eq. (20) is not equivalent to the full set of ideal MHD equations. Since it contains some of the same physics, and has some analogous behavior, it is a worthwhile approximation for the study of flux emergence which cannot be studied in any other way.

DWL would like to thank G. H. Fisher, M. G. Linton, R. C. Canfield and A. A. Pevtsov for useful discussions. We thank the anonymous referee for helpful comments on the manuscript. DWL was supported by NAGW-5072.

A. Evaluating stresses, torques and angular momenta

The cross-sectional stress $\mathbf{N}$ and torque $\mathbf{M}$ involve integrals over the magnetic field in the flux tube. The details of these field, which we call the tube's *profile*, have been left unspecified in most of this work. Here we will make an assumption that the detailed form of the magnetic field profile is determined entirely by the *configuration* of the tube's axis $\mathbf{x}(\ell)$. This is to say that the profiles do not involve the tube's instantaneous velocity or acceleration, $\dot{\mathbf{x}}(\ell)$ or $\ddot{\mathbf{x}}(\ell)$. For treatment of the profile we will adopt quasi-cylindrical internal coordinates $\mathbf{r}_\perp = (\varpi, \phi)$ within the cross section $\Sigma(\ell)$. The angle ϕ is measured from the Frenet normal vector $\hat{\mathbf{n}}$ if it is defined, otherwise the value of ϕ is not relevant.

As a starting point we consider the tube with it's axis straightened out, and assume the profile to be axisymmetric $B_\ell(\varpi)$, $B_\phi(\varpi)$. Because $\beta \gg 1$ there are no constraints on these functions from force-balance; any radial magnetic force will be balanced by pressure with a negligible distortion of the tube's interior. The assumption of uniform twist, however, imposes the constraint $B_\phi(\varpi) = q\varpi B_\ell(\varpi)$. This assumption has greatly simplified the kinematics of the tube, and it eliminates the possibility of such purely internal dynamics as internal kinking (Linton et al. 1996). As a result we have one function $B_\ell(\varpi)$ which is entirely arbitrary.

The profile is axisymmetric when the axis is straight, but departures from straightness (e.g. curvature) will introduce an asymmetry. Following this reasoning, the parallel component of the field has the form

$$B_\ell(\varpi, \phi) = B_\ell^{(0)}(\varpi) \; + \; B_\ell^{(1)}(\varpi, \phi) \quad , \tag{A1}$$

where $B_\ell^{(1)}$ must vanish with the tube's curvature κ, and $B_\ell^{(0)}(\varpi)$ is the arbitrary

function defining the profile. Adopting κa as the formal ordering parameter we expect to leading order $B_\ell^{(1)}/B_\ell^{(0)} \sim \mathcal{O}(\kappa a)$. This formal ordering will be maintained throughout even though there are some applications where κa will be close to unity.

Bending a segment of tube may cause an overall increase in length which can change $B_\ell^{(0)}$; however, it will also cause differential changes in length over the cross section. These differential changes make the outside longer and the inside shorter (see fig. 1). Absence of cross-sectional shear implies that for a tube with curvature κ the region at position (ϖ, ϕ) lengthens by a factor $1 - \kappa\varpi\cos(\phi)$. Recall that $\phi = 0$ corresponds to the inside of the curve (i.e. the $\hat{\mathbf{n}}$ direction), where the tube shortens. For flux tubes in the solar corona the pressure balance, eq. (13), is dominated by the gas pressure ($\beta \gg 1$) so local changes such as bending will occur almost incompressibly. Therefore the parallel expansion must be compensated by a lateral compression of perpendicular areas by a factor $1 + \kappa\varpi\cos(\phi)$. (This will be accompanied by a displacement of the central axis by $\sim \kappa a^2$, which we ignore). Conservation of flux dictates that $[1 + \kappa\varpi\cos(\phi)]B_\ell = \text{const.}$ so

$$B_\ell^{(1)}(\varpi, \phi) \;\simeq\; -\kappa\varpi\cos(\phi)\, B_\ell^{(0)}(\varpi) \quad . \tag{A2}$$

Thus the parallel field is enhanced on the outside of the tube ($\phi = \pi$) and reduced on the inside ($\phi = 0$). This is opposite to the tendency of force-free magnetic fields ($\beta \ll 1$).

In one term in N_ℓ it is possible for a second order contribution, $B_\ell^{(2)}$ to appear. There is, however, an arbitrary component of the perpendicular incompressible distortions which enters at this order. This makes it impossible to derive a unique form for $B_\ell^{(2)}$. We will therefore choose to omit it entirely. Its contribution would be $\mathcal{O}(\kappa^2 a^2)$ in a term already containing $\mathcal{O}(1)$ terms so we do not believe that dropping the term will change the fundamental physics.

A twisted magnetic flux tube will also have an azimuthal field component B_ϕ. We have assumed uniform twist, i.e.,

$$B_\phi(\varpi) = q\varpi\, B_\ell^{(0)}(\varpi) \quad , \tag{A3}$$

for an uncurved axis. We will use the formal ordering of a weakly twisted tube $qa \ll 1$ (Linton et al. 1996), although this will once again be violated in certain circumstances. In a tube which is both twisted and bent B_ϕ will also develop a ϕ dependence, however, this contribution will be $\mathcal{O}(q\kappa a^2)$ and we will neglect it. The final field component B_ϖ will appear implicitly, but is not needed for our calculations.

Using the above expressions for B_ℓ in the equation for stress, eq. (16), gives

$$\begin{aligned} N_\ell &= \frac{1}{4\pi}\int_0^{2\pi} d\phi \int_0^a \varpi\, d\varpi\, [B_\ell^{(0)}(\varpi)]^2\, [1 + \kappa\varpi\cos(\phi)]^2 \\ &= \frac{A\bar{B}^2}{4\pi}\left[\,\gamma_0 + \tfrac{1}{2}\kappa^2 a^2 \gamma_2\,\right] \quad . \end{aligned} \tag{A4}$$

In writing the final expression we have used the average field strength $\bar{B}(\ell) = \Phi/A(\ell)$ where Φ is the net (axial) flux in the tube. We have also introduced the factors γ_n which describe moment $n+1$ of the field profile

$$\gamma_n \equiv \frac{n+2}{a^{n+2}} \int_0^a \left[\frac{B_\ell^{(0)}(\varpi)}{\bar{B}} \right]^2 \varpi^{n+1}\, d\varpi \quad , \tag{A5}$$

normalized to be unity for a flat profile, $B_\ell^{(0)}(\varpi) = \bar{B}$. These factors depend only on the shape of the profile. Maintaining pressure balance in the face of a large value of β requires fluid to expand or contract homologously, for instance as the tube rises into regions of lower pressures. A homologous expansion or contraction would change the tube's radius without altering the shapes of any field profiles, thus factors γ_n will be constant in time. Assuming the tube had an initially uniform profile then $\partial_\ell \gamma_n = 0$ and the factors can be considered scalar parameters of the problem. In full MHD treatments the shape of the profile has an affect on stability and growth rates (Linton et al. 1996).

To calculate the cross sectional torque we first use the local Frenet vectors to write

$$\mathbf{r}_\perp = \varpi \left[\cos(\phi)\, \hat{\mathbf{n}} \; + \; \sin(\phi)\, \hat{\mathbf{b}} \right] \quad , \quad \hat{\boldsymbol{\phi}} = -\sin(\phi)\, \hat{\mathbf{n}} \; + \; \cos(\phi)\, \hat{\mathbf{b}} \quad . \tag{A6}$$

Performing the integration in eq. (23) yields

$$\mathbf{M} = \frac{\gamma_2 \Phi^2}{8\pi^2} \left[q(\ell)\, \hat{\mathbf{l}} \; + \; \kappa(\ell)\, \hat{\mathbf{b}} \right] \quad , \tag{A7}$$

where all the l dependence appears inside the square brackets.

Next, we evaluate the angular momentum (per unit mass) $\mathbf{L}$. In general, the tube segment V has the angular velocity (cf. eq. [2])

$$\boldsymbol{\Omega} = \omega \hat{\mathbf{l}} \; + \; \hat{\mathbf{l}} \times \frac{d\hat{\mathbf{l}}}{dt} \quad ,$$

about its center of mass. Assuming a circular cross section, the moment of inertia about $\hat{\mathbf{l}}$ is

$$I_\ell \;=\; 2\pi \bar{\rho} \frac{a^4}{4}\, d\ell \;=\; \tfrac{1}{2} a^2\, \bar{\rho} A\, d\ell \quad .$$

About the axes perpendicular to $\hat{\mathbf{l}}$ and in the limit $d\ell \to 0$ (i.e. a flat disk), the moment of inertia is

$$I_\perp \;=\; \bar{\rho} \frac{\pi a^4}{4}\, d\ell \;=\; \tfrac{1}{4} a^2 \bar{\rho} A\, d\ell \quad .$$

Combining these with the definition of $\mathbf{L}$ yields

$$\mathbf{L} = \frac{A}{2\pi} \left(\omega \hat{\mathbf{l}} \; + \; \tfrac{1}{2} \hat{\mathbf{l}} \times \frac{d\hat{\mathbf{l}}}{dt} \right) \quad . \tag{A8}$$

REFERENCES

Batchelor, G. K. 1967, Fluid Dynamics (Cambridge: Cambridge Univ. Press)

Berger, M. A., & Field, G. B. 1984, JFM, 147, 133

Caligari, P., Moreno-Insertis, F., & Schüssler, M. 1995, ApJ, 441, 886

Calugareanu, G. 1961, Czechoslovak Math J., 11, 588

Cheng, J. 1992, A&A, 264, 243

Chou, D.-Y., & Fisher, G. H. 1989, A&A, 341, 533

Choudhuri, A. R. 1990, A&A, 239, 335

Choudhuri, A. R., & Gilman, P. A. 1987, ApJ, 316, 788

Dichmann, D. J., & Maddocks, J. H. 1996, J. Nonlin. Sci., To appear

D'Silva, S., & Choudhuri, A. R. 1993, A&A, 272, 621

Fan, Y., Fisher, G. H., & DeLuca, E. E. 1993, ApJ, 405, 390

Fan, Y., Fisher, G. H., & McClymont, A. N. 1994, ApJ, 436, 907

Ferriz-Mas, A., & Schussler, M. 1990, in Geophys. Monographs, Vol. 58, Physics of Magnetic Flux Ropes, ed. C. T. Russel, E. R. Priest, & L. C. Lee (AGU), 141

Fisher, G. H., Fan, Y., & Howard, R. F. 1995, ApJ, 438, 463

Klapper, I. 1996, J. Comp. Phys., 125, 325

Klapper, I., & Tabor, M. 1994, J. Phys. A, 27, 4919

Lau, Y.-T. 1995, Phy. Plasmas, 2, 4442

Leka, K. D., Canfield, R. C., McClymont, A. N., & Van Driel Gesztelyi, L. 1996, ApJ, 462, 547

Linton, M. G., Longcope, D. W., & Fisher, G. H. 1996, ApJ, 469, 954

Longcope, D. W., & Fisher, G. H. 1996, ApJ, 458, 380

Longcope, D. W., Fisher, G. H., & Arendt, S. 1996, ApJ, 464, 999

Moffatt, H. K. 1978, Magnetic Field Generation in Electrically Conducting Fluids (Cambridge: Cambridge University Press)

Moffatt, H. K., & Ricca, R. L. 1992, Proc. Roy Soc. Lond. A, 439, 411

Moreno-Insertis, F. 1986, A&A, 166, 291

Moreno-Insertis, F., & Emonet, T. 1996, ApJ, 472, L53

Parker, E. 1975, ApJ, 198, 205

Parker, E. N. 1979, Cosmical Magnetic Fields, Their Origin and Their Activity (Oxford: Clarendon Press)

Pevtsov, A. A., Canfield, R. C., & Metcalf, T. R. 1995, ApJ, 440, L109

Pohl, W. F. 1968, J. Math. Mech., 17, 975

Priest, E. R. 1982, Solar Magnetohydrodynamics, Vol. 21 (Boston: D. Reidel)

Schüssler, M. 1979, A&A, 71, 79

Spruit, H. C. 1981, A&A, 98, 155

Tanaka, K. 1991, Solar Phys., 136, 133

Tsinganos, K. 1980, ApJ, 239, 746

White, J. H. 1969, Am. J. Math., 91

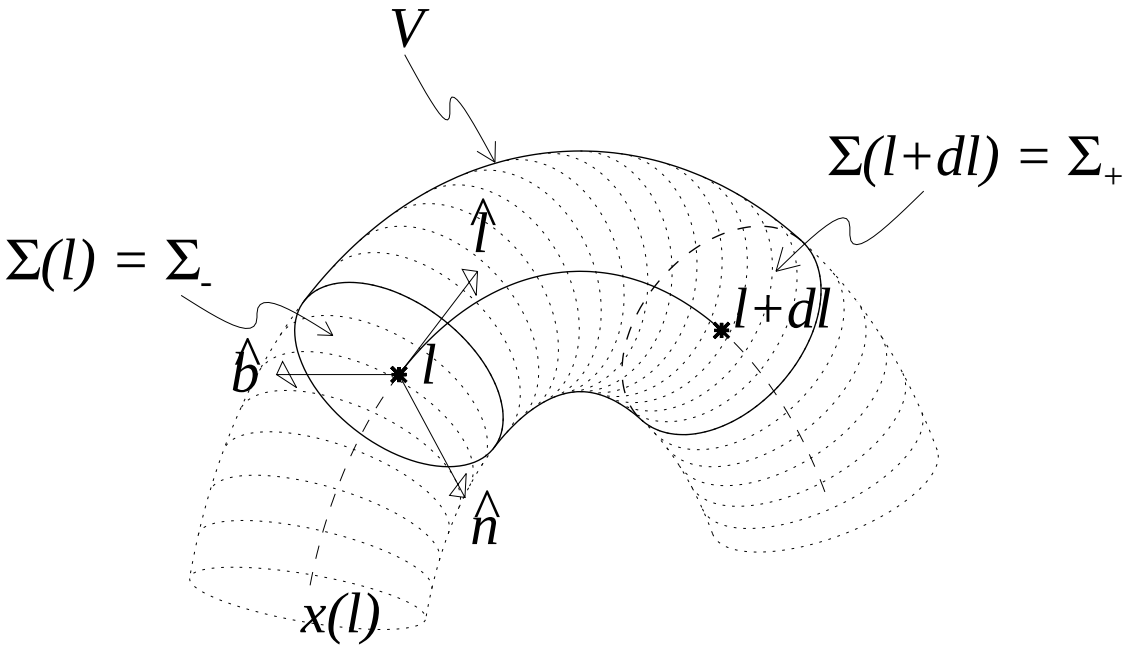

Fig. 1.— A segment of the flux tube V. Dotted lines indicate a portion of the arched tube, while the solid lines outline the segment V. The axis $\mathbf{x}(\ell)$ is shown as a solid and dashed line. V encompasses the segment $(\ell, l + d\ell)$ and is bounded by the cross sections $\Sigma(\ell)$ and $\Sigma(\ell + d\ell)$. The Frenet coordinates $\hat{\mathbf{l}}$, $\hat{\mathbf{n}}$ and $\hat{\mathbf{b}}$ are also shown.

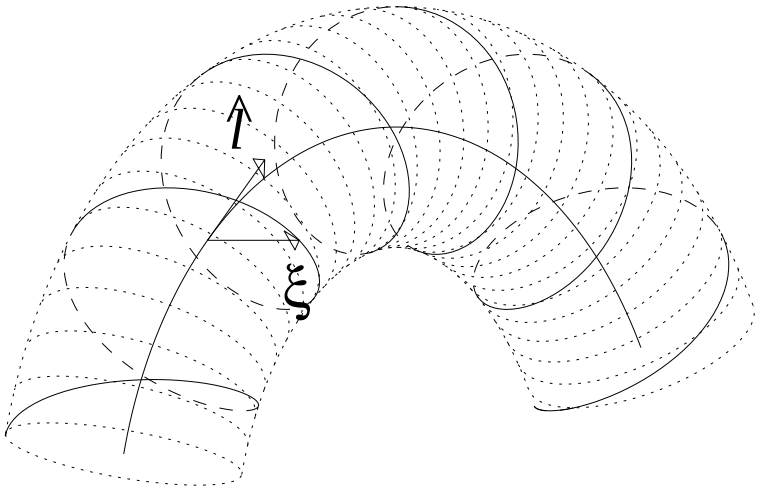

Fig. 2.— The same section of tube shown in fig. 1 showing the twisted field lines and the unit vectors $\hat{\mathbf{l}}$ and $\boldsymbol{\xi}$.

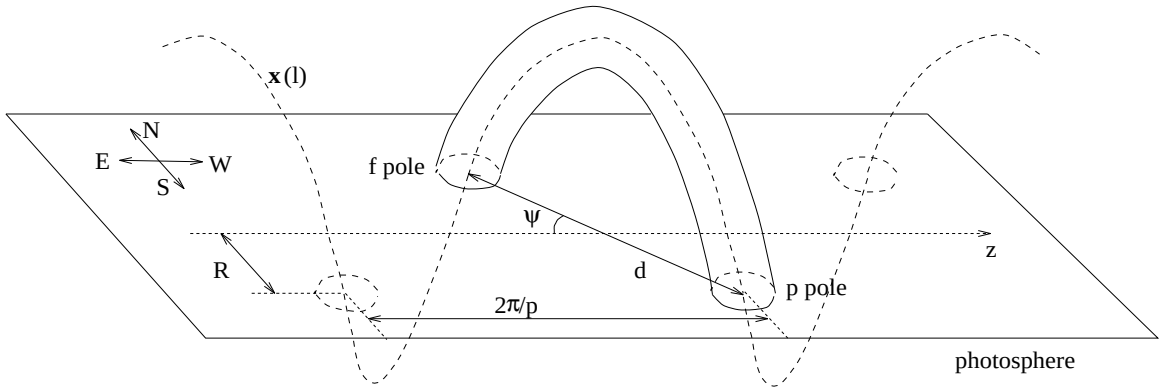

Fig. 3.— A section of helical flux tube used to model an emerged bipole. The axis of the helix, with pitch p and amplitude R, is shown as a dashed line. The axis of the helix, the z axis, lies on the photospheric plane oriented along the E-W direction. Its intersection with the photosphere forms the (leading) p-pole and (following) f-pole of the bipole. The bipole has a separation d and a tilt angle ψ.

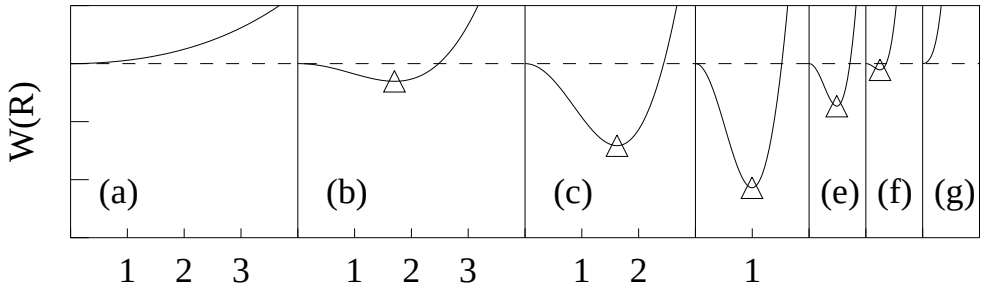

Fig. 4.— The potential $W(R)$ plotted versus $Q_0 R$ for a tube with $Q = 4$, and values of $\tilde{p}$ of (a) 0.1, (b) 0.2, (c) 0.3, (d) 0.5, (e) 0.7, (f) 0.8 and (f) 0.9. Equation (58) dictates that the $R = 0$ state is unstable for $0.15 < \tilde{p} < 0.85$ corresponding to (b)–(f). In those cases the minimum R^* is shown with a triangle. A constant value has been subtracted from each curve to make $W(0) = 0$.

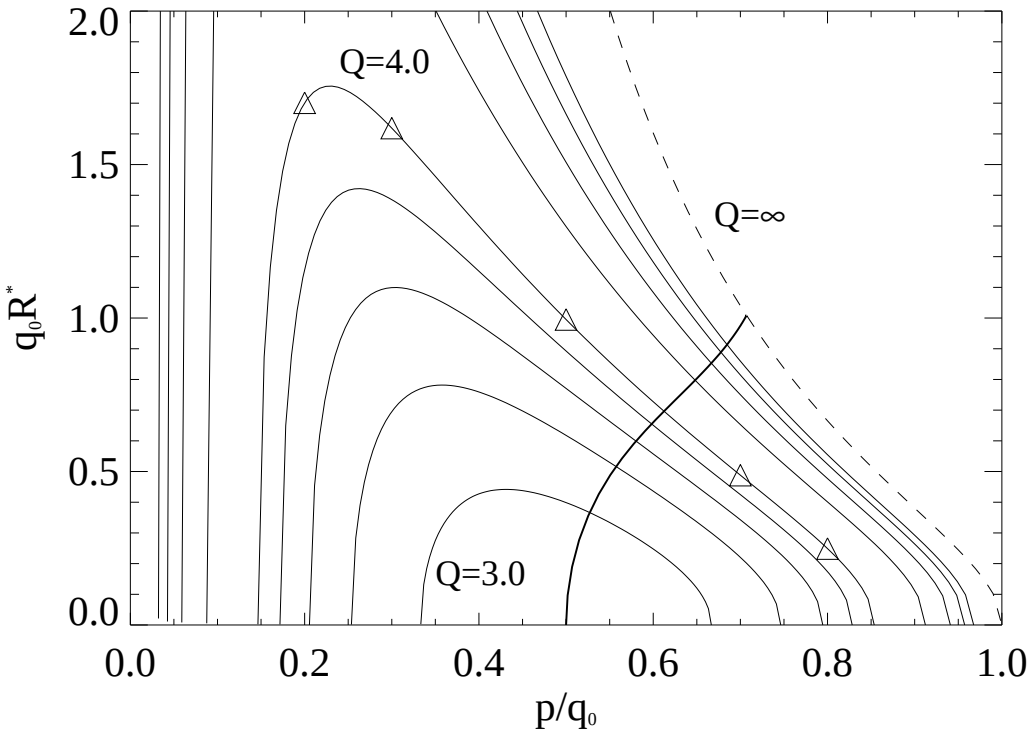

Fig. 5.— The normalized equilibrium amplitude q_0R^* plotted against $\tilde{p}$ for tubes with Q = 3.0, 3.25, 3.5, 3.75, 4.0, 5.0, 6.0, 7.0, 8.0 (solid) and the limiting case $Q = \infty$ (dashed). The five points shown in fig. 4 (i.e. $\tilde{p}$ = 0.2, 0.3, 0.5, 0.7, 0.8 for Q = 4.0) are shown as triangles. The values of q_0R^* for the points of maximum growth, $\tilde{p}_{\max}(Q)$, are shown as a dark solid line.